



ORIGINAL ARTICLE

Organic acid catalyzed production of platform chemical 5-hydroxymethylfurfural from fructose: Process comparison and evaluation based on kinetic modeling

Muhammad Sajid ^{a,b,c,1}, Yuchen Bai ^{a,b}, Dehua Liu ^{a,b}, Xuebing Zhao ^{a,b,*}

^a Key Laboratory of Industrial Biocatalysis, Ministry of Education, Tsinghua University, Beijing 100084, China

^b Institute of Applied Chemistry, Department of Chemical Engineering, Tsinghua University, Beijing 100084, China

^c Department of Chemical Engineering, University of Gujrat, Gujrat 50700, Pakistan

Received 7 June 2020; accepted 18 August 2020

Available online 27 August 2020

KEYWORDS

5-Hydroxymethylfurfural (HMF);
Organic acids;
Fructose;
Dehydration;
Kinetic modeling

Abstract Fructose was converted to 5-hydroxymethylfurfural (HMF), an important biomass-derived platform chemical, under mild conditions (100–130 °C) with several organic acids including *p*-toluene sulfonic (*p*TSA), oxalic, maleic, malonic and succinic acids as the catalysts. The process kinetics was compared considering fructose dehydration to HMF as the objective reaction and condensation of fructose and HMF to humin and rehydration of HMF as the main side reactions. DMSO was found to be the most effective solvent reaction medium to obtain high fructose conversion and HMF yield. Observed kinetic modeling illustrated that the rehydration and condensation of HMF in DMSO actually could be neglected, especially for the oxalic acid catalyzed system. The determined observed activation energy for fructose conversion to HMF and humin in DMSO medium was 33.75 and 24.94 kJ/mol for *p*TSA catalyzed system, and 96.51 and 78.39 kJ/mol for oxalic acid-catalyzed system, respectively. HMF yields of 90.2% and 84.1% were obtained for *p*TSA and oxalic acid catalyzed systems, respectively.

© 2020 The Author(s). Published by Elsevier B.V. on behalf of King Saud University. This is an open access article under the CC BY-NC-ND license (<http://creativecommons.org/licenses/by-nc-nd/4.0/>).

* Corresponding author at: Key Laboratory of Industrial Biocatalysis, Ministry of Education, Tsinghua University, Beijing 100084, China.

E-mail address: zhaorb@mails.tsinghua.edu.cn (X. Zhao).

¹ ORCID - 0000-0001-9471-8395.

Peer review under responsibility of King Saud University.



Production and hosting by Elsevier

1. Introduction

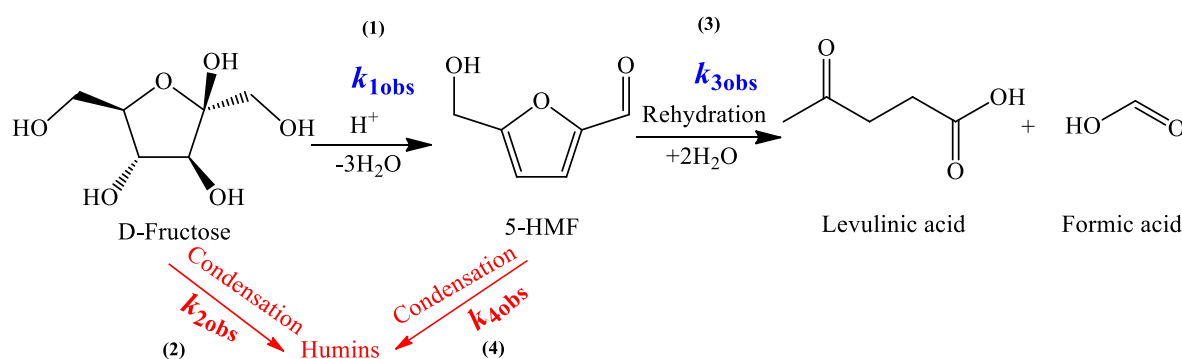
Exhaustion of fossil resources has compelled extensively for the manufacture of “green” chemicals from biomass resources (Chaudhary et al., 2020; Van Putten et al., 2013; Wang et al., 2017). The applications of furan derivatives from carbohydrates has been acknowledged with a relatively long history (Clarke et al., 2018). Commercial production of furfural has been well achieved from agricultural residues such as corncob

(Zhang et al., 2017). The process proceeds by hydrolysis of pentosans in the biomass to monosaccharides (pentoses) followed by dehydration to furan aldehydes (van Dam et al., 1986). 5-Hydroxymethylfurfural (HMF) is another important member of the biomass-derived furan family due to its multifunctionality (Zhang and Huber, 2018). It has two dissimilar functional groups attached at the *para* position that increases the variety of its derivatives (Wang et al., 2017). Due to its versatile usability, the US Department of Energy also acknowledges HMF as one of the top 30 chemicals (Werpy and Peterson, 2004). Numerous furan derivatives can be produced by the oxidation of HMF comprising 2,5-diformylfuran (DFF), 5-hydroxymethyl-2-furancarboxylic acid (HFCA), 5-formylfuran-2-carboxylic acid (FFCA), and the most important is 2,5-furandicarboxylic acid (FDCA) (Galkin and Ananikov, 2019; Sajid et al., 2018). Particularly, FDCA can be used as a monomer for the synthesis of green bio-based polymer polyethylene 2,5-furandicarboxylate (PEF) which is alternative to the fossil-based terephthalic acid (TPA) derived polyethylene terephthalate (PET) with significant features like outstanding gas barrier performance, recyclability and exceptional mechanical properties (Sajid et al., 2018).

Fructose has been successfully dehydrated to HMF by acid catalysts, using conventional heating and microwave irradiation (Wrigstedt et al., 2016) in different systems such as water (Antonetti et al., 2019), organic (Hu et al., 2013), biphasic (Wrigstedt et al., 2016), ionic liquids (Hu et al., 2013), and deep eutectic solvents (Zuo et al., 2017) with homogeneous or heterogeneous catalysts (Wang et al., 2019) via the reaction route shown in Scheme 1. It can be validated that the pH value, as well as the acid itself, plays a key role in the formation mechanism of HMF. Mineral acids can facilitate fructose dehydration and have been used successfully for decades (Garcés et al., 2017; Rosatella et al., 2011). However, increasing environmental concerns has compelled to replace these mineral acids with organic acids or other catalysts having lower toxicity and high biodegradability (Yu and Tsang, 2017). Oxalic acid, formic acid, and acetic acid have been used for fructose dehydration to HMF for 2,5-bis(hydroxymethyl) furan (BHMF) production and 99% HMF yield was attained in DMSO system (Thananathanachon and Rauchfuss, 2010). Lactic acid, formic acid, and acetic acid were also applied as catalysts for fructose dehydration and a maximum HMF yield of 64% was obtained with lactic acid (50 wt%) in 2 h at 150 °C using an autoclave (Souza et al., 2012). An increase in the acid concentration of acetic acid and formic acid improved the fruc-

tose conversion but decreased the HMF selectivity. Kinetic study of the process indicates the increasing trend of side reactions (humin formation) with an increase in the acidity of the system (Souza et al., 2012; Takeuchi et al., 2008).

Comparative analysis of different catalytic systems is very difficult if reaction kinetics under certain environments is not developed (Zhao et al., 2017). Investigation on kinetic modeling can contribute to sketching the true descriptive conclusion on the definite impacts of the catalyst, reaction rate, and product quantification. Kinetics of fructose dehydration with high pressure reactor was investigated by Bicker et al. (2005) in supercritical methanol and supercritical acetic acid using sulfuric acid (0.01 M) as the catalyst. Later, Asghari and Yoshida (2007) also investigated the kinetics of fructose dehydration to HMF and HMF rehydration to LA/FA in sub-critical water. They concluded that the formation of by-products was also from HMF along with fructose in the sub-critical water system. They developed an independent kinetic model for the quantitative comparison of condensation products from fructose and HMF. The kinetic parameters obtained from the anticipated reaction path divulged a good agreement with experimental results (Asghari and Yoshida, 2007). Similarly, Nikbin et al. (2012), described his finding using hybrid quantum mechanics/molecular mechanics free energy calculations to evaluate the reaction mechanism for fructose dehydration to HMF in acidulated water. What has been investigated so far is majorly focused on the potential influence of the nature of Brønsted acid used and the effect of initial pH on the dehydration mechanisms. Comparison of different Brønsted acids such as sulfuric acid, phosphoric acid, hydrochloric acid, and nitric acid have been well performed (Körner et al., 2018; Takeuchi et al., 2008). However, how organic acid catalysts affect the kinetics of fructose dehydration has not been well elucidated. Therefore, in this work, several organic acids, especially dicarboxylic acids (DCAs) were used for the dehydration of fructose to produce HMF in water and DMSO medium. A comparison with the case of using *p*-toluenesulfonic acid (*p*TSA) based on the observed kinetic modeling results was further made. DCAs usually have enough acidity, but the acidity is not as strong as sulfuric acid, and therefore the decomposition of fructose and HMF would be alleviated. Furthermore, DCAs show sensitive response to temperature on its solubility in water, and therefore, recovery of the DCAs is possible by cooling the solution and crystallization (Chen et al., 2017). Moreover, organic acids are usually good solvents to lignin, a polymeric component of lignocellu-



Scheme 1 Major reactions involved in fructose dehydration to HMF over acid catalyst.

losic biomass, due to its acidity and strong hydrogen bonding ability (Zhao et al., 2017). Therefore, the DCA-catalyzed system may achieve a good fractionation of lignocellulosic biomass with the simultaneous conversion of the polysaccharides to furan compounds such as furfural (from xylan) and HMF (from glucan) in a one-pot process. The objective of this work is to make quantitative evaluation and comparison of several organic acids catalyzed production of HMF from fructose based on kinetic modeling, which is one of the most important steps for conversion of lignocellulosic biomass to HMF. The obtained results may not only provide the observed kinetic data on various organic acid catalyzed conversion of fructose to HMF but also serve as a powerful tool to further optimize and control the process to maximize HMF yield and minimize the formation of by-products.

2. Experimental

2.1. Chemicals and materials

Fructose (>99.5%), *p*-toluene sulfonic acid (*p*TSA, 99.5%), oxalic acid (99.5%), maleic acid (99.5%), malonic acid (97%), and succinic acid (99.5%) were purchased from Shanghai Aladdin Biotechnology Co., Ltd., China. Dimethyl sulfoxide (DMSO, 99.8%), N, N-dimethylformamide (DMF, 99%), and isopropyl alcohol (IPA, 99.7%) were purchased from Beijing chemical works, Beijing, China. Polyethylene glycol with different molecular weight (PEG-400, PEG-1000, PEG-2000, ≥97%) were purchased from Beijing Tongguang Fine Chemical Company, China. The analytical standard 5-hydroxymethyl furfural (HMF, 99%), levulinic acid (LA, 97.5%), formic acid (FA, 96%), and fructose (>99.9%) were purchased from Shanghai Aladdin Biotechnology Co., Ltd., China. Ultra-pure water (double deionized water, DDIW) of 18.25 Mega ohm (MΩ) resistivity was prepared in the lab.

2.2. Dehydration of fructose to 5-hydroxymethylfurfural

The required amount (molar) of fructose was dissolved in 50 ml water or organic solvent in a 100 ml three-neck round bottom flask equipped with total reflux. The required amount (molar) of the catalyst was also added to the flask and mixed thoroughly. *p*TSA ($pK_{a1} = -2.8$), oxalic acid ($pK_{a1} = 1.27$), maleic acid ($pK_{a1} = 1.9$), malonic acid ($pK_{a1} = 2.83$) and succinic acid ($pK_{a1} = 4.2$) were used as organic acid catalysts. Temperature was continuously observed throughout the reaction process. A magnetic stirrer was used for keeping homogenous mixing and uniform temperature distribution. The mixed solution was heated in an oil bath at different temperatures for required time with continuous stirring. Samples were collected with a predetermined time interval and cooled quickly in an ice-cooled water bath to terminate the reaction. These samples are then preserved in a refrigerator for future analysis.

2.3. Analytical methods

2.3.1. Determination of the products concentrations

The concentration of fructose, HMF, levulinic acid, and formic acid were determined by HPLC analysis performed with

a SHIMADZU HPLC system (SHIMADZU, Japan) equipped with an Aminex® HPX-87H strong acid cation exchange resin column (300 × 7.8 mm, Bio-Rad, USA) at 65 °C with a RID-10A differential refractive index detector. Fructose, HMF, Levulinic acid, and formic acid analyses were performed with the same column with 5 mM sulfuric acid solution as the eluent at a flow rate of 0.8 ml min⁻¹. Before HPLC analysis, the samples were diluted with ultra-pure water and filtered through a 0.22-μm syringe filter. The injection volume was 20 micro liter (μl) per analysis and auto-injection module was applied.

To evaluate the reaction efficiency for HMF production from fructose, several parameters were defined, including fructose conversion (X_{FRU}), yield of HMF (Y_{HMF}), yield of levulinic acid (Y_{LA}), yield of formic acid (Y_{FA}), selectivity of HMF (S_{HMF}) and carbon balance (CB) were calculated based on the subsequent equations (Eqs. (1)–(4)). Carbon balance was used to determine the amount of side products called humin (HUM) (Steinbach et al., 2018):

Fructose conversion (X_{FRU})

$$= \left[1 - \frac{\text{Fructose molar concentration}}{\text{Initial fructose molar concentration}} \right] \times 100 \quad (1)$$

Product yield (Y_P)

$$= \left[\frac{\text{Product (HMF/LA/FA) molar concentration}}{\text{Initial fructose molar concentration}} \right] \times 100 \quad (2)$$

$$\text{HMF selectivity } (S_{HMF}) = \left[\frac{\text{HMF yield } (Y_{HMF})}{\text{Fructose conversion } (X_{FRU})} \right] \times 100 \quad (3)$$

Carbon balance (CB) = ($6 \times X_{FRU}$)

$$- [(6 \times Y_{HMF}) + (5 \times Y_{LA}) + (1 \times Y_{FA})] \quad (4)$$

2.3.2. Development of the observed kinetic models

Fructose dehydration is a complex reaction with multiple steps. Fructose dehydration to HMF is influenced by the competitive reaction of fructose isomerization to glucose, condensation to disaccharides, and dehydration to anhydrosugars (Akien et al., 2012; Kimura et al., 2013). Similarly, produced HMF undergoes rehydration to LA/FA as well as dimerization/condensation to multiple products summarized as humin (Desir et al., 2019; Kimura et al., 2013). Side reactions are usually unavoidable and how these reactions proceed during the process are complicated. Therefore, all these unwanted side reactions either from fructose or from HMF are summarized as “humin formation” (Steinbach et al., 2018). Based on this assumption, the reactions taking place in the system can be simplified as shown in Scheme 1, and plausible reaction mechanism of acid catalyzed dehydration of fructose to HMF is provided in supporting information Fig. S1, in which H⁺ catalyzes the reaction process in three steps by removing one molecule of water in each step. Following observed homogeneous kinetic models (Eqs. (5)–(8)) were thus could be devel-

oped by assuming that all these reactions are first-order with respect to the corresponding reactants:

$$-\frac{dC_{\text{FRU}}}{dt} = (k_{1\text{obs}} + k_{2\text{obs}})C_{\text{FRU}} \quad (5)$$

$$\frac{dC_{\text{HMF}}}{dt} = k_{1\text{obs}}C_{\text{FRU}} - (k_{3\text{obs}} + k_{4\text{obs}})C_{\text{HMF}} \quad (6)$$

$$\frac{dC_{\text{LA/FA}}}{dt} = k_{3\text{obs}}C_{\text{HMF}} \quad (7)$$

$$\frac{dC_{\text{HUM}}}{dt} = k_{2\text{obs}}C_{\text{FRU}} + k_{4\text{obs}}C_{\text{HMF}} \quad (8)$$

where, $k_{1\text{obs}}$, $k_{2\text{obs}}$, $k_{3\text{obs}}$, and $k_{4\text{obs}}$ are the observed rate constants for fructose dehydration to HMF, decomposition/condensation of fructose to humin, rehydration of HMF to LA/FA and condensation of HMF to humin, respectively. Humin is the condensation product and its concentration was calculated by the difference between fructose conversion and recorded reaction products based on mass balance (Steinbach et al., 2018). C_{FRU} , C_{HMF} , $C_{\text{LA/FA}}$, and C_{HUM} are the molar concentrations of corresponding substrates and products, respectively.

Based on the observed kinetic model presented above, the analytical solution for fructose concentration and HMF concentration can be calculated by the integration forms as Eqs. (9) and (10), respectively (Körner et al., 2018). The detailed derivation is provided as supporting information Scheme S1.

$$C_{\text{FRU}} = C_{\text{FRU}(0)} e^{-(k_{1\text{obs}}+k_{2\text{obs}})t} \quad (9)$$

$$C_{\text{HMF}} = \left[\frac{k_{1\text{obs}}C_{\text{FRU}(0)}}{-k_{1\text{obs}} - k_{2\text{obs}} + k_{3\text{obs}} + k_{4\text{obs}}} (e^{(-k_{1\text{obs}}-k_{2\text{obs}}+k_{3\text{obs}}+k_{4\text{obs}})t} - 1) + C_{\text{HMF}(0)} \right] e^{-(k_{3\text{obs}}+k_{4\text{obs}})t} \quad (10)$$

2.3.3. Data processing and fitting of kinetic parameters

The fitting of observed kinetic parameters including rate constants, activation energy etc. were performed based on experimental data using MATLAB R2016a software by numerical integration of Eqs. (5)–(8) with ode45 function and then optimized by least square method. The observed activation energy E_a and Arrhenius factor A were calculated using an extended Arrhenius equation with MATLAB R2016a software.

3. Results and discussion

3.1. Dehydration of fructose to HMF in an aqueous system

Adoption of water as a reaction medium for a chemical reaction is always the first choice due to its neutral behavior, versatility, and eco-friendly nature. Water is a cheap and green solvent with bulk availability and high solubility of sugars (Yoshida, 2006). Therefore, fructose dehydration to HMF in water system with organic acid catalysts was firstly performed at 100 °C as shown in supporting information Fig. S2 for the time courses of fructose conversion, HMF, and LA yields. *p*TSA showed the highest reaction rate for fructose conversion, but the rate of HMF rehydration to form formic and levulinic acids also proceeded quickly thus lowering HMF yield in the

late phase of the reaction. This was primarily because *p*TSA has the highest acidity ($\text{p}K_{\text{a}1} = -2.8$) than other organic acids. Oxalic acid ($\text{p}K_{\text{a}1} = 1.27$) also showed good catalytic efficiency for fructose dehydration, and the HMF yield and selectivity were even higher than *p*TSA. However, maleic acid, malonic acid, and succinic acid showed much poorer fructose conversion, though maleic acid obtained similar HMF yield at the 12th hour of reaction. Particularly, succinic acid showed the lowest HMF yield and selectivity probably due to its weakest acidity. Although increasing acidity could result in increase in fructose dehydration in aqueous media, the relationship between $\text{p}K_{\text{a}1}$ of the acids and fructose conversion and HMF yields seemed not to be simply linear. Surely there were several other factors contributing to the dehydration process (van Dam et al., 1986).

It was also observed that the nature of the acid catalyst affects the color of the solution by the formation of different side products during the reaction. Akien et al.(2012), Antal et al. (1990) and many others (Antonetti et al., 2019; Heo et al., 2019; Kimura et al., 2013) briefly described the mechanism of fructose dehydration with competitive isomerization, fragmentation, and condensation. Reported results elucidated that acid strength, acid concentration, and nature of the solvent are crucial factors and play a key role in the determination of fructose conversion route (Akien et al., 2012; Antonetti et al., 2019; Takeuchi et al., 2008). It has been observed that moderate acids are more selective than strong mineral acids because of the superiority of reaction of fructose dehydration to HMF over fructose decomposition/condensation reactions (Antal et al., 1990; Antonetti et al., 2019; Heo et al., 2019; Takeuchi et al., 2008). Fine tuning of strong acids in a narrow range is vital for formation of the objective product (HMF) whereas higher concentrations lead to HMF rehydration and condensation (Akien et al., 2012; Takeuchi et al., 2008). The dehydration of fructose to HMF is a multistep process (see supporting information Fig. S1), disturbing the product balance at initial stage which results in an increased humin calculation along with the side product formations (Kimura et al., 2013). With consideration of the catalytic behavior and catalysis superiority in aqueous phase fructose dehydration results, oxalic acid and *p*TSA appeared to be more promising catalyst candidates for fructose dehydration.

The observed kinetics of the organic acid-catalyzed dehydration of fructose in water medium was further investigated based on the aforementioned kinetic models (Eqs. (5)–(8)) with experiment-determined data. The model and experiment-predicted reaction curves are shown in Fig. 1. Corresponding fitted rate constants and goodness of fit (R^2) are listed in Table 1. The results suggested that the model-predicted data generally had good accordance with the experimental results with most of R^2 being ≥ 0.9 , indicating that the developed kinetic models were applied to the reaction system. However, it should be noted that humin looks increasing quickly at the early stage of reaction, especially for the *p*TSA-catalyzed system, and relatively high deviation between model-predicted data and “experimental” data. This was primarily because the humin concentration was calculated according to carbon balance and thus some possible intermediates such as glucose formed by fructose isomerization, disaccharide formed by fructose and anhydrosugar formed by dehydration of fructose were also counted as humin. Nevertheless, humin is not the objective product, and it is still feasible to consider all the

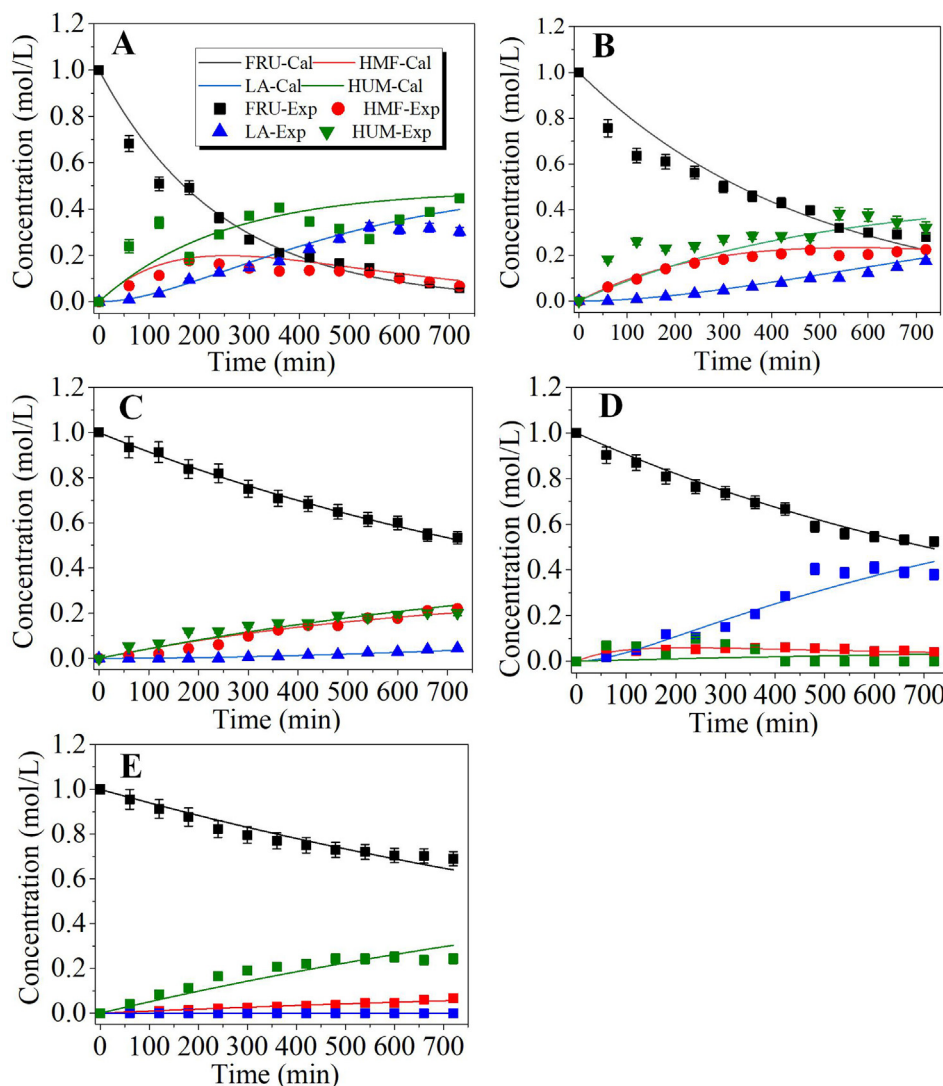


Fig. 1 Kinetic plots of different organic acids catalyzed conversion of fructose in water medium. Reaction conditions: 1.0 M Fructose with 1.0 M acid catalysis in 50 ml deionized water at 100 °C with stirring rate of 200 rpm for 12 h. (A) *p*TSA; (B) oxalic acid; (C) maleic acid; (D) malonic acid; and (E) succinic acid. Lines are for model-predicted data, and symbols are for experiment-determined data. FRU: fructose; HMF: 5-hydroxymethylfurfural; LA: levulinic acid; HUM; humin.

Table 1 Fitted kinetic rate constants for organic acid-catalyzed dehydration of fructose to HMF in water medium. The initial fructose and acid catalyst concentrations were 1.0 M.

Acid catalyst	Temp (°C)	Observed rate constant (min ⁻¹)				Goodness of Fit (<i>R</i> ²)		<i>Y</i> _{HMF} %
		<i>k</i> _{1obs}	<i>k</i> _{2obs}	<i>k</i> _{3obs}	<i>k</i> _{4obs}	Fructose	HMF	
<i>p</i> TSA	100	2.1 × 10 ⁻³	1.97 × 10 ⁻³	3.7 × 10 ⁻³	4.4 × 10 ⁻¹³	0.9576	0.9247	17.7 ± 2.1
Oxalic acid	100	1.1 × 10 ⁻³	9.7 × 10 ⁻⁴	1.5 × 10 ⁻³	4.2 × 10 ⁻¹⁴	0.9525	0.9849	23.3 ± 1.2
Maleic acid	100	4.5 × 10 ⁻⁴	4.5 × 10 ⁻⁴	4.2 × 10 ⁻⁴	1.1 × 10 ⁻¹²	0.9948	0.9243	22.1 ± 1.1
Malonic acid	100	9.2 × 10 ⁻⁵	6.0 × 10 ⁻⁵	1.2 × 10 ⁻⁴	5.2 × 10 ⁻¹³	0.9667	0.8909	8.0 ± 1.2
Succinic acid	100	9.7 × 10 ⁻⁵	5.2 × 10 ⁻⁵	5.4 × 10 ⁻⁸	1.3 × 10 ⁻¹²	0.9479	0.9291	6.6 ± 1.0

non-objective products as humin in an observed kinetic modeling. As shown in Table 1, both *k*_{1obs} and *k*_{2obs} had values in the range of 10⁻⁵–10⁻³ min⁻¹, while *k*_{3obs} varied in a wider range of 10⁻⁸–10⁻³ min⁻¹ depending on the catalyst used.

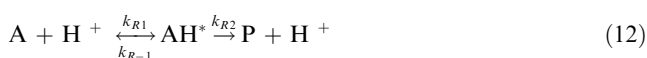
However, *k*_{4obs} were much smaller than *k*_{1obs}, *k*_{2obs}, and *k*_{3obs}, indicating that the consumption of HMF in the system was primarily due to the rehydration reaction. Zhang et al., (2016) evaluated the kinetic study of aqueous phase glucose

dehydration to HMF using a combination of AlCl_3 with HCl and maleic acid. The results demonstrated that glucose dehydration proceeded via the isomerization of glucose to fructose followed by the dehydration of fructose to HMF, so their data in principle is comparable with our results. Although the magnitude of rate constants was much higher because of the high reaction temperature (140 °C–180 °C); however, the trend was similar. The rate of HMF rehydration to LA/FA was higher (0.03–0.11 min^{-1}) than that of HMF condensation to humin (0.01–0.06 min^{-1}) (Zhang et al., 2016). Similarly, (Körner et al., 2018) studied the aqueous phase fructose dehydration at 140 °C. Although the used reaction parameters (high temperature and Brønsted acids) were different, the HMF consumption trend was quite similar to the finding of this work. At this temperature, they found that the rate of HMF rehydration to LA/FA was higher than the rate of HMF degradation to humin. At pH 1.2, HCl and HNO_3 gave the HMF rehydration rates of $23.5 \times 10^{-3} \text{ min}^{-1}$ and $24.16 \times 10^{-3} \text{ min}^{-1}$ and rates of HMF degradation to humin of $3.5 \times 10^{-3} \text{ min}^{-1}$ and $2.99 \times 10^{-3} \text{ min}^{-1}$, respectively (Körner et al., 2018). Hence, the results of this work and reported ones indicated that the consumption of HMF in the system was primarily due to the rehydration reaction, especially at low temperatures. It was also demonstrated from Table 1 that the rates of fructose dehydration to HMF ($k_{1\text{obs}}$) followed the order of $p\text{TSA} > \text{oxalic acid} > \text{maleic acid} > \text{malonic acid} > \text{succinic acid}$. However, the condensation reaction of fructose to humin ($k_{2\text{obs}}$) generally followed the same order too, and so did the rehydration of HMF ($k_{3\text{obs}}$), except that malonic acid unpredictably showed higher value of $k_{3\text{obs}}$. The above results revealed that the rates of both the objective reactions (fructose dehydration to HMF) and side reactions (rehydration and condensation of HMF) increased with the acidity strength of the organic acid catalysts, indicating that these reactions could be promoted by proton (H^+). Similar behavior was also observed by other researchers when Brønsted acids were used as catalysts (Körner et al., 2018; Yoshida, 2006).

For interpretation of the possible mechanisms, it was assumed that first-order rate equations could be used for the conversion of reactant A to product P as $\text{A} \rightarrow \text{P}$ for fructose dehydration with an apparent differential reaction rate of

$$\frac{d[\text{P}]}{dt} = k_R[\text{A}] \quad (11)$$

where k_R is the observed rate constant. By considering the effect of homogenous catalyst and introducing the effect of proton, following kinetic model can be assumed (Espenson, 1981):



where k_{R1} is the rate of formation of acid-catalyzed intermediate complex AH^* , which is also typically known as the protonation of the reactant, k_{R-1} is rate constant for the reverse reaction of protonation, and k_{R2} is the rate of formation of product (P). Furthermore, by assuming quasi-stationary for $[\text{AH}^*]$, ordinary differential equations thus can be obtained as follows:

$$-\frac{d[\text{A}]}{dt} = k_{R1}[\text{A}][\text{H}^+] - k_{R2}[\text{AH}^*] \quad (13)$$

$$\frac{d[\text{AH}^*]}{dt} = k_{R1}[\text{A}][\text{H}^+] - (k_{R2} + k_{R-1})[\text{AH}^*] = 0 \quad (14)$$

$$\frac{d[\text{P}]}{dt} = k_{R2}[\text{AH}^*] \quad (15)$$

According to Eq. (14), it can be obtained that

$$k_{R1}[\text{A}][\text{H}^+] = (k_{R2} + k_{R-1})[\text{AH}^*] \quad (16)$$

namely $[\text{AH}^*] = \frac{k_{R1}}{(k_{R2} + k_{R-1})}[\text{A}][\text{H}^+]$. The Eq. (15) thus can be expressed as

$$\frac{d[\text{P}]}{dt} = k_{R2} \frac{k_{R1}}{(k_{R2} + k_{R-1})}[\text{A}][\text{H}^+] \quad (17)$$

It thus can be obtained for the relationship between the apparent rate constant k_R and proton concentration as

$$k_R = \frac{k_{R1}k_{R2}}{k_{R2} + k_{R-1}}[\text{H}^+] \quad (18)$$

Eq. (18) represents a linear dependency of k_R on proton concentration $[\text{H}^+]$. $p\text{TSA}$ has a very negative pK_{a1} value (−2.8), and it can be considered to completely dissociate in an aqueous system. For other carboxylic acid, the H^+ ($[\text{H}^+]$) concentration in its aqueous solution can be estimated by the following equation (Sun et al., 2011);

$$[\text{H}^+] \approx \sqrt{C_A K_{a1}} \quad (19)$$

where C_A is the concentration of the organic acid catalysts. Therefore, the $[\text{H}^+]$ of the system at room temperature with an initial acid concentration of 1.0 M could be approximately estimated as 1, 0.232, 0.112, 0.038, and 0.008 M for $p\text{TSA}$, oxalic acid, maleic acid, malonic acid and succinic acid, respectively. Plots of these estimated $[\text{H}^+]$ with the determined values of $k_{1\text{obs}}$ as shown in Fig. 2 gave a good linear relationship ($R^2 = 0.9804$) for these organic acids except $p\text{TSA}$. The deviation of $p\text{TSA}$ from the linear plots might be due to the too high acid concentration (1.0 M). However, these results indicated that the organic acid catalyzed dehydration of fructose generally followed the proposed mechanisms illustrated as reaction Eq. (12) with protonation as the first step. Körner et al. (2018) also observed a similar trend in Brønsted acid catalyzed dehydration of fructose to HMF. However, it should be noted that pK_{a1} of the dicarboxylic acid used is also impacted by temperature, and more details should be further investigated with consideration of the temperature effects.

The data listed in Table 1 also demonstrates that $p\text{TSA}$ and oxalic acid were better catalysts than other acids for fructose conversion. However, the rate constants of fructose condensation to humin ($k_{2\text{obs}}$) and HMF to LA and FA ($k_{3\text{obs}}$) were also large leading to poor selectivity and HMF yield. Defining selectivity for fructose conversion (S_F) as $k_{1\text{obs}}/k_{2\text{obs}}$. It could be obtained that the S_F for $p\text{TSA}$, oxalic acid, maleic acid; malonic acid, and succinic acid were 1.07, 1.13, 1.0, 1.53 and 1.86, respectively. The relatively low selectivity was not only ascribed to the catalyst properties but also strongly related to the reaction medium. Particularly, when water was used as the medium, the rehydration reaction definitely could be promoted because the water was also a reactant. Therefore, the rehydration of HMF had a comparable apparent rate constant ($k_{3\text{obs}}$) to the condensation of fructose ($k_{2\text{obs}}$), suggesting

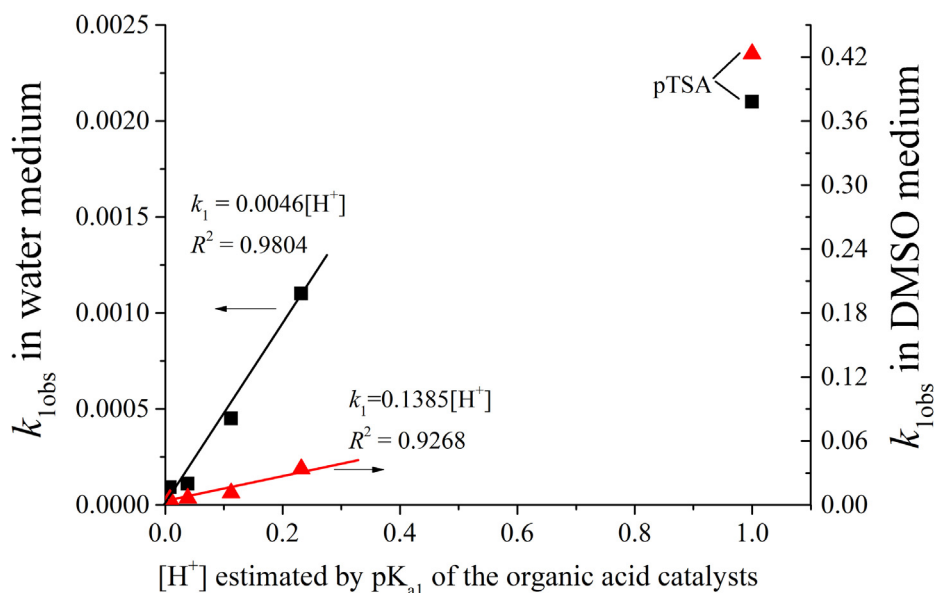


Fig. 2 Plots of $[H^+]$ (H^+ concentration) estimated by pK_{a1} (pK_a) values of the used organic acid catalysts with experiment-determined k_{1obs} in water or DMSO medium.

that the non-objective consumption of fructose was contributed by both reactions. Anyway, the above results revealed that water was not a good reaction medium for HMF production, and the organic solvent system might increase the selectivity and HMF yield.

3.2. Dehydration of fructose in organic solvent medium

Several organic solvents including DMSO, DMF, IPA, PEG-400, PEG-1000, and PEG-2000 were selected as reaction medium with consideration of their high boiling-point and fructose-dissolving capacity (Dalessandro and Pliego, 2018; Gajula et al., 2017; Mellmer et al., 2018). Since oxalic acid and *p*TSA gave relatively higher HMF yields (18–23%) when applied in a water medium, they were further used for solvent screening. The kinetic plots of experimental data and model-predicted curves are provided in Fig. 3, and fitted rate constants are shown in Table 2, which demonstrated that the developed model similarly could well describe the trends of fructose conversion and formation of various products. Corresponding product yield and HMF selectivity for certain reaction time are provided in supporting information Table S1.

The results indicated that the fructose conversion and HMF selectivity was indeed greatly dependent on the solvent medium used. Compared with those obtained in the water medium, the HMF decomposition product LA/FA was dramatically reduced in most of the selected solvents and HMF yield could be greatly increased, especially in DMSO medium. The maximum HMF yield reached about 80% with 80.3% selectivity after reaction for seven hours with oxalic acid as the catalyst at 110 °C. Similar HMF yield and selectivity of 79% were also obtained with *p*TSA as the catalyst in DMSO medium with similar parameters in less time. The data are shown in Table 2 clearly indicated that DMSO medium could obtain much larger rate constants for fructose conversion (k_{1obs} and k_{2obs}), and the corresponding selectivity for fructose conversion ($S_F = k_{1obs}/k_{2obs}$) increased to 2.60 and 2.61 for

oxalic acid and *p*TSA catalysts, respectively, in comparison to about 1 for water medium. The results also revealed that the reaction rates for rehydration of HMF (k_{3obs}) were greatly reduced in most solvent mediums, compared with that in a water medium. This was because, in the solvent mediums, much less water was present in the system and thus the apparent rate constants were greatly reduced. The rate of HMF condensation to humin (k_{4obs}) was also greatly dependent on the solvent used. However, in most cases, it was much lower than other rate constants. For example, in DMSO system, k_{3obs} were lower than k_{1obs} and k_{2obs} by three orders of magnitude while k_{4obs} lower by nine orders of magnitude, which suggested that rehydration and condensation of HMF in DMSO system actually could be neglected. Therefore, DMSO has been selected as the most effective solvent medium for acid-catalyzed conversion of fructose to HMF.

The effects of different organic acid catalysts on HMF production in DMSO medium were further investigated. The kinetic curves of the concentrations of fructose and different products are provided in Fig. 4, and the corresponding fitted rate constants are listed in Table 3. The results again indicated that the model could be used to describe the kinetics of organic acid-catalyzed dehydration of fructose in DMSO medium with most of R^2 being higher than 0.95. The fitted rate constants revealed that the rate of fructose dehydration catalyzed by these organic acids followed the order of *p*TSA > oxalic acid > maleic acid > succinic acid > malonic acid, which was similar to that in a water medium. However, the values of k_{1obs} were in the range of 10^{-3} – 10^{-1} min^{-1} and generally larger than those obtained in the water system. Corresponding selectivity for fructose conversion (k_{1obs}/k_{2obs}) was determined to be 2.61, 2.60, 1.62, 0.90 and 8.3, respectively. The anomaly observed with malonic acid (as S_F increased from 1.53 to 8.3) is partly due to the inductive effect, medium acid strength, and partly due to the autocatalysis of produced LA/FA which promotes the fructose dehydration being the moderate acids (Antal et al., 1990; Gawade and Yadav, 2018). Villanueva

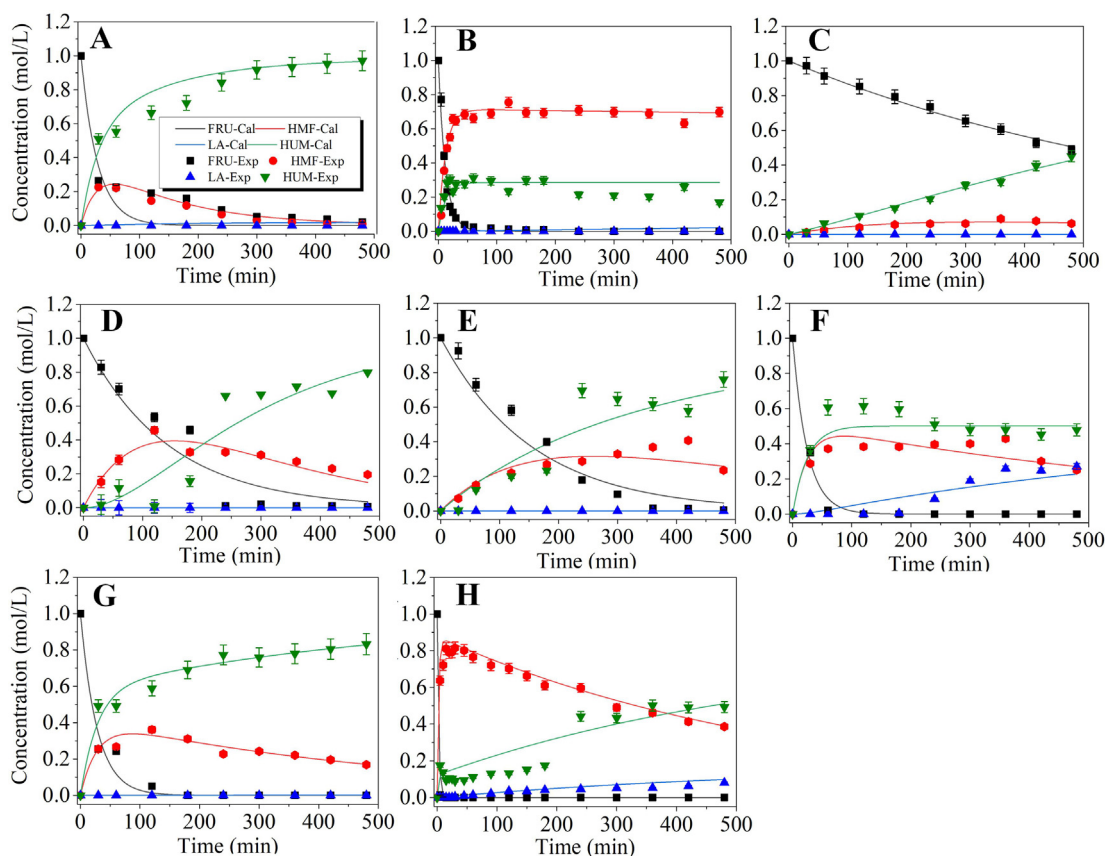


Fig. 3 Kinetic plots of oxalic acid and *p*TSA catalyzed conversion of fructose in different solvent medium. Reaction conditions: 1.0 M acid catalyst and with 1.0 M fructose in 50 ml solvent heated in oil bath for 8 h with a stirring speed of 200 rpm; the flask was heated in oil bath at 100 °C for water medium, at 110 °C for DMSO, DMF and IPA medium, and at 120 °C for PEG-400, PEG-1000 and PEG-2000 medium. (A) oxalic acid in DMF; (B) oxalic acid in DMSO; (C) oxalic acid in IPA; (D) oxalic acid in PEG-400; (E) oxalic acid in PEG-1000; (F) oxalic acid in PEG-2000; (G) *p*TSA in IPA (H) *p*TSA in DMSO. Lines are for model-predicted data, and symbols are for experiment-determined data. FRU: fructose; HMF: hydroxymethylfurfural; LA: levulinic acid; HUM; humin.

Table 2 Kinetic parameters for oxalic acid and *p*TSA-catalyzed conversion of fructose to produce HMF in different solvent medium. Reaction conditions: 1.0 M acid catalyst and with 1.0 M fructose in 50 ml solvent heated in oil bath for certain time with a stirring speed of 200 rpm; the flask was heated in oil bath at 100 °C for water medium, at 110 °C for DMSO, DMF and IPA medium, and at 120 °C for PEG-400, PEG-1000 and PEG-2000 medium.

Solvent	Catalyst	Temp (°C)	Observed rate constant (min ⁻¹)				Goodness of Fit (<i>R</i> ²)		<i>Y</i> _{max} %
			<i>k</i> _{1obs}	<i>k</i> _{2obs}	<i>k</i> _{3obs}	<i>k</i> _{4obs}	Fructose	HMF	
DMF	Oxalic acid	110	1.2×10^{-2}	2.2×10^{-2}	3.5×10^{-4}	6.6×10^{-3}	0.9607	0.9528	16.3 ± 1.1
DMSO	Oxalic acid	110	0.0339	0.0130	7.5×10^{-11}	2.8×10^{-14}	0.9852	0.9503	79.8 ± 0.5
IPA	Oxalic acid	110	6.2×10^{-4}	8.1×10^{-4}	2×10^{-9}	5.4×10^{-3}	0.993	0.8718	9.1 ± 0.8
PEG-400	Oxalic acid	120	6.9×10^{-3}	7.3×10^{-10}	9.2×10^{-10}	5.9×10^{-3}	0.9255	0.8522	45.8 ± 1.1
PEG-1000	Oxalic acid	120	3.5×10^{-3}	3.0×10^{-3}	4.9×10^{-10}	2.1×10^{-3}	0.9069	0.8066	40.7 ± 1.2
PEG-2000	Oxalic acid	120	0.021	0.021	1.3×10^{-3}	5.1×10^{-14}	0.9924	0.8183	42.9 ± 0.9
Water	Oxalic acid	100	1.1×10^{-3}	9.7×10^{-4}	1.5×10^{-3}	4.2×10^{-14}	0.9525	0.9849	23.3 ± 1.2
IPA	<i>p</i> TSA	110	3.1×10^{-3}	1.5×10^{-3}	4.4×10^{-3}	8.1×10^{-12}	0.9723	0.9218	36.1 ± 0.8
DMSO	<i>p</i> TSA	110	0.4231	0.1624	1.5×10^{-4}	3.3×10^{-10}	0.9881	0.9732	79.0 ± 1.3
Water	<i>p</i> TSA	100	2.1×10^{-3}	1.97×10^{-3}	3.7×10^{-3}	4.4×10^{-13}	0.9576	0.9247	17.7 ± 2.0

and Marzialetti (2018) studied the fructose dehydration over solid phosphate catalyst and found that the rate constants of fructose conversion to HMF (*k*_{1obs}) were $1.28 \times 10^{-2} \text{ min}^{-1}$, $1.69 \times 10^{-2} \text{ min}^{-1}$ and $3.3 \times 10^{-2} \text{ min}^{-1}$ at 125 °C, 135 °C,

and 145 °C (Villanueva and Marzialetti, 2018). They also assumed that there was no degradation of HMF so *k*_{3obs} and *k*_{4obs} were not calculated, hence the fructose conversion selectivity was very high (29.76, 18.98 and 20.62, respectively);

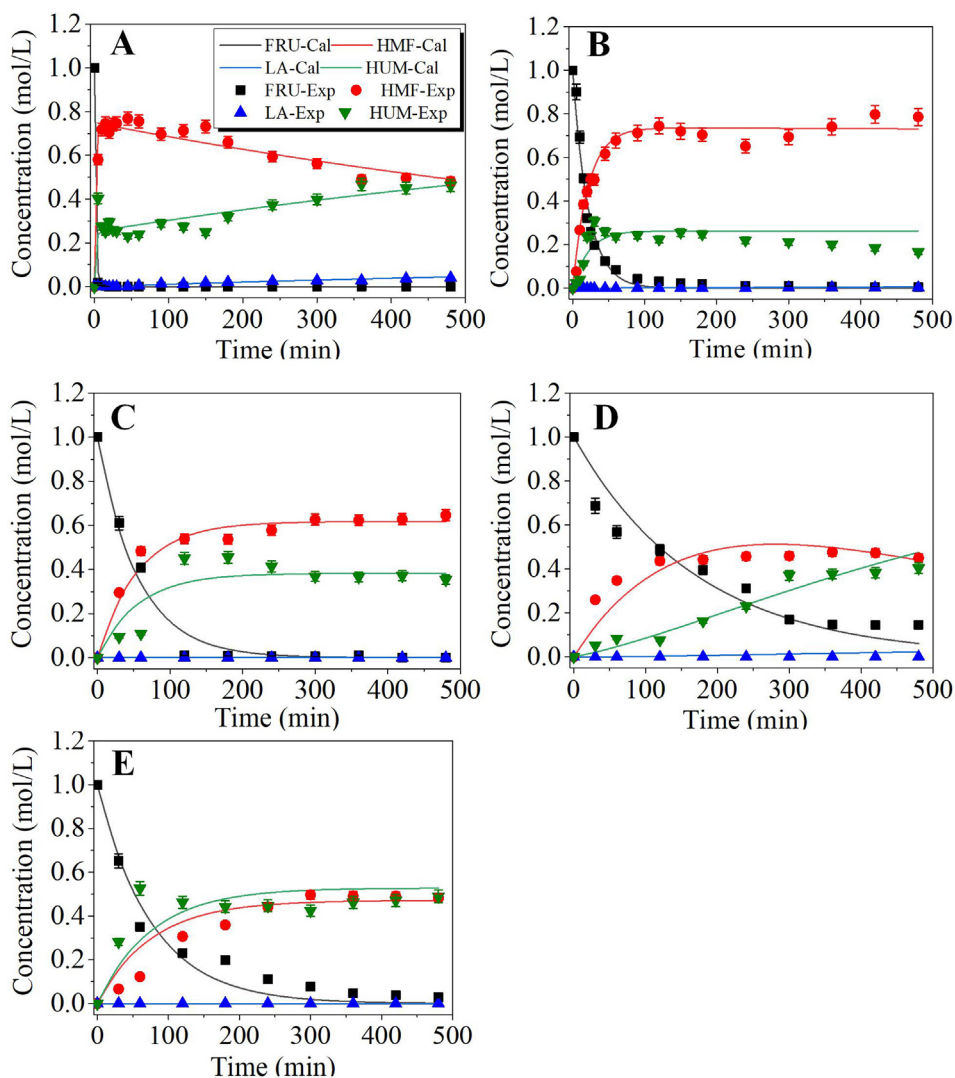


Fig. 4 Kinetic plots of different organic acids catalyzed conversion of fructose in DMSO medium. Reaction conditions: 1.0 M Fructose with 1.0 M acid catalyst in 50 ml DMSO heated in an oil bath at 110 °C with stirring speed of 200 rpm for 8 h. (A) *p*TSA; (B) oxalic acid; (C) maleic acid; (D) succinic acid and (E) malonic acid. Lines are for model-predicted data, and symbols are for experiment-determined data. FRU: fructose; HMF: 5-hydroxymethylfurfural; LA: levulinic acid; HUM; humin.

Table 3 Fitted observed kinetic constants of organic acid-catalyzed conversion of fructose in DMSO medium. Reaction conditions: 1.0 M Fructose with 1.0 M acid catalyst in DMSO medium heated in an oil bath at 110 °C with stirring rate of 200 rpm for 8 h.

Catalyst	Observed rate constant (min^{-1})				Goodness of Fit (R^2)		X_F (%)	Max. Y_{HMF} (%)
	$k_{1\text{obs}}$	$k_{2\text{obs}}$	$k_{3\text{obs}}$	$k_{4\text{obs}}$	Fructose	HMF		
<i>p</i> TSA	0.4231	0.1624	1.5×10^{-4}	3.3×10^{-10}	0.9985	0.9586	100	79.8 ± 1.1
Oxalic acid	0.0339	0.0130	7.5×10^{-11}	2.8×10^{-14}	0.9808	0.9867	100	79.0 ± 0.5
Maleic acid	0.0112	6.9×10^{-3}	3.4×10^{-12}	2.2×10^{-14}	0.9842	0.9694	99.4 ± 1.2	68.0 ± 1.0
Succinic acid	6.2×10^{-3}	6.9×10^{-3}	3.3×10^{-10}	2.2×10^{-14}	0.9688	0.8481	91.2 ± 1.1	49.7 ± 1.2
Malonic acid	5.2×10^{-3}	6.3×10^{-4}	1.13×10^{-4}	1.87×10^{-3}	0.9484	0.8852	85.1 ± 2.1	47.7 ± 0.7

Körner et al. (2018) also studied the fructose dehydration over organic and Brønsted acid catalysts using a micro autoclave. The rate constants for fructose conversion to HMF ($k_{1\text{obs}}$) were 2.08 min^{-1} , 0.6 min^{-1} , and 0.76 min^{-1} for citric acid ($\text{pH}_{\text{RT}} = 2.0$), glycolic acid ($\text{pH}_{\text{RT}} = 1.8$) and acetic acid

($\text{pH}_{\text{RT}} = 2.0$), respectively. The fructose conversion selectivity ($k_{1\text{obs}}/k_{2\text{obs}}$) was 3.65, 1.88, and 2.0, respectively, at 140 °C. Although the applied temperature and pressure (140 °C and autogenous pressure) were higher than those used in the system of this work, the fructose conversion selectivity was com-

parable. When the pH of the citric acid catalyzed process increased from 1.4 to 2.0, the $k_{1\text{obs}}$ decreased from 2.08 min^{-1} to 0.72 min^{-1} showing the H^+ dependency of the fructose dehydration process. When Brønsted acids including H_3PO_4 (pH = 1.0), HNO_3 (pH = 1.2) and H_2SO_4 (pH = 1.1) were applied, the observed $k_{1\text{obs}}$ were 10.2 min^{-1} , 4.532 min^{-1} and 3.35 min^{-1} , respectively. This dramatical change in $k_{1\text{obs}}$ at a relatively similar pH validated the effect of the type of acids on the fructose dehydration reaction.

Being like the water-medium dehydration, the observed rate of fructose dehydration generally increased with the increase in the $\text{pK}_{\text{a}1}$ value of the organic acids, suggesting that the acidity of the system played a vital role for fructose dehydration. $k_{1\text{obs}}$ similarly showed a good ($R^2 = 0.9268$) linear relationship with $[\text{H}^+]$ estimated by the $\text{pK}_{\text{a}1}$ of the dicarboxylic acids (Fig. 2). The maximal HMF yields obtained during the dehydration process were in the range of 47–80% with corresponding fructose conversion of 85–100% under the employed conditions as shown in Table 3. Oxalic acid and *p*TSA obtained the maximal HMF yield with 80.3% and 79% HMF selectivity, respectively at 110 °C with a substrate to catalyst ratio of 1. However, oxalic acid catalyzed conversion needed much longer reaction time (7 h) to achieve the maximal HMF yield compared with *p*TSA-catalyzed system (0.5 h) at the same temperature employed (110 °C). Prolonging reaction time significantly increased the formation of humin, with a notable decrease in HMF concentration, but LA concentration just slightly increased (Fig. 3A). However, no apparent increase in humin and LA concentrations was observed after 120 min when oxalic acid was used as the catalyst (Fig. 3B). Anyway, DMSO medium could obtain greatly improved HMF yield and selectivity over the water medium system. This was primarily achieved by reducing the formation of degradation products such as levulinic and formic acids, and could be reflected by the fact that the rate constants for rehydration of HMF ($k_{3\text{obs}}$) in DMSO medium was about 1–8 orders of magnitude smaller than those obtained in a water medium. One of the primary reasons for this phenomenon might be the presence of little water in the DMSO system, which eventually reduces the apparent rate of HMF rehydration. Moreover, probably the solvation effects of DMSO towards the reactants and products might also contribute to decelerating the side reactions.

3.3. Maximizing HMF yield and selectivity for *p*TSA and oxalic acid catalyzed process in DMSO medium

3.3.1. *p*TSA catalyzed system

Other process parameters such as temperature and catalyst concentration were further optimized at atmospheric pressure in DMSO medium. The reaction temperature was regulated from 100 °C to 130 °C and substrate to catalyst ratio (S/C) from 0.5 to 2 M/M. The fructose conversion sharply increased with the reaction time and almost reached 100% with a maximum HMF yield at 30 min for *p*TSA-catalyzed system. The maximum HMF yield (90.2%) was obtained at 120 °C with 0.5 M/M S/C. Rapid fructose conversion with *p*TSA was mainly attributed to its higher acidity ($\text{pK}_{\text{a}1} = -2.8$) and ionization potential at the reaction temperature. However, after this, the effects of time were negative and rehydration/condensation of HMF prevailed with an increasing trend as indicated by a gradual decrease in HMF yield and selectivity. The initial

fructose concentration also demonstrated significant effects on fructose conversion, HMF yield, and selectivity as shown in supporting information Fig. S3. For the *p*TSA-catalyzed system, the fructose conversion reached ~100% no matter what the initial fructose concentration was; however, increasing fructose concentration resulted in a gradually decrease in the levels of HMF yield and selectivity. For example, the HMF yield decreased from 90.2% to 62.1% when the initial fructose concentration increased from 0.5 M to 2.0 M. This was probably because the reaction rates of side reactions might become more significantly enhanced at a high fructose concentration.

The observed kinetics of *p*TSA-catalyzed dehydration of fructose at an initial fructose concentration of 1.0 M with varied *p*TSA concentration (0.5–2.0 M) at different temperatures were further investigated. The fitted observed rate constants are shown in Table 4. The results illustrated that the developed kinetic model could well describe the kinetics of the system. All the plots showed that temperature had an important influence on the HMF yield and the formation of humin and HMF degradation products. This was proved by the fact that the HMF concentration increased with time and decreased after reaching a maximum, especially at reaction temperatures of higher than 120 °C. All the rate constants increased with reaction temperature and *p*TSA concentration. The objective reaction (dehydration of fructose to HMF) had the largest rate constant ($k_{1\text{obs}}$), but the rate constant of the main side reaction, namely condensation of fructose to humin ($k_{2\text{obs}}$) had somewhat smaller values than $k_{1\text{obs}}$, but they were still in the same order of magnitude. The reactions for HMF rehydration and condensation proceeded at much lower rates, which was reflected by the result that $k_{3\text{obs}}$ and $k_{4\text{obs}}$ were smaller by 2–12 orders of magnitude depending on the reaction temperature and acid concentration. Only at a high temperature, for example, at 130 °C, the rehydration and condensation of HMF became significant, but the rate constants were still smaller than $k_{2\text{obs}}$ by two orders of magnitude. The change of $k_{3\text{obs}}$ and $k_{4\text{obs}}$ values in a wide range of the order of magnitude suggested that HMF rehydration and condensation had very large activation energy, namely, the temperature would show a very significant influence on these side reactions. Therefore, to obtain the maximum HMF yield, the effects of temperature on both the objective and side reactions should be considered. For example, low temperature may reduce the formation of condensation products, but the rate of fructose dehydration might be too small leading to long reaction time and low HMF yield; however, the too high temperature could greatly reduce reaction time but might lead to the formation of more condensation products. Similar temperature effects were also observed by Alexandra et al.,(2017).

Based on the fitted observed rate constants, fructose conversion selectivity ($S_{\text{F}} = k_{1\text{obs}}/k_{2\text{obs}}$) and HMF consumption selectivity ($S_{\text{HMF}} = k_{3\text{obs}}/k_{4\text{obs}}$) was calculated and listed in Table 4. The results similarly revealed that S_{F} generally increased with temperature increase but decreased at 130 °C. S_{F} was also affected by *p*TSA concentration. The highest S_{F} was generally obtained at 110–120 °C with 0.5–1.0 M *p*TSA concentration. Contrarily, S_{HMF} increased from 100 °C to 110 °C and then decreased. This indicates that decomposition of HMF to humin increased beyond 110 °C and at 100–110 °C, rehydration of HMF to LA/FA was the major consumption route. For a more comprehensive comparison, the experiment-determined maximum HMF yield (Y_{HMF}) and

Table 4 Fitted observed rate constants for *p*TSA-catalyzed dehydration of fructose to HMF in DMSO medium at different temperature with varied catalyst concentration. The initial fructose concentration was fixed at 1.0 M.

<i>p</i> TSA conc. (M)	Temp (°C)	Observed rate constant (min ⁻¹)				Goodness of Fit (R ²)	S _F	S _{HMF}	Max. Y _{HMF} (%)	t _{opt} (h)	
		k _{1obs}	k _{2obs}	k _{3obs}	k _{4obs}						Fructose
0.5	100	0.2091	0.0820	6.7 × 10 ⁻¹³	1.5 × 10 ⁻¹³	0.9983	0.9121	2.55	4.47	78.6 ± 1.2	2.5
	110	0.3929	0.1006	9.8 × 10 ⁻⁸	2.2 × 10 ⁻¹⁴	0.999	0.9549	3.91	2.2 × 10 ⁶	76.5 ± 0.8	1.5
	120	0.4577	0.1190	2.1 × 10 ⁻⁴	9.8 × 10 ⁻⁴	0.997	0.9405	3.85	0.22	80.1 ± 1.1	0.5
	130	0.4630	0.1370	4.93 × 10 ⁻⁴	5.17 × 10 ⁻⁴	0.9995	0.9831	3.38	0.96	81.0 ± 0.9	0.5
1.0	100	0.2304	0.0959	1.17 × 10 ⁻¹⁰	3.33 × 10 ⁻¹²	0.9594	0.9368	2.40	35.14	75.8 ± 2.0	1.0
	110	0.4231	0.1124	1.5 × 10 ⁻⁴	3.28 × 10 ⁻¹⁰	0.9985	0.9586	3.76	4.5 × 10 ⁵	76.8 ± 1.8	0.75
	120	0.5634	0.1561	8.29 × 10 ⁻⁴	3.35 × 10 ⁻⁴	0.9881	0.9732	3.61	2.47	81.5 ± 0.9	0.5
	130	0.6139	0.1682	5.56 × 10 ⁻⁴	2.53 × 10 ⁻³	0.9998	0.977	3.65	0.22	77.9 ± 1.3	0.5
1.5	100	0.2394	0.1083	2.1 × 10 ⁻¹³	2.2 × 10 ⁻¹⁴	0.9988	0.9194	2.21	9.55	83.3 ± 1.0	1.5
	110	0.4362	0.1569	2.9 × 10 ⁻⁴	2.0 × 10 ⁻¹⁰	0.9992	0.9015	2.78	1.4 × 10 ⁶	85.8 ± 0.8	1.5
	120	0.5616	0.2088	7.8 × 10 ⁻⁴	9.8 × 10 ⁻⁴	0.9999	0.9629	2.69	0.796	74.7 ± 0.9	10(min)
	130	0.5424	0.2298	1.2 × 10 ⁻³	2.5 × 10 ⁻³	0.9995	0.9657	2.36	0.48	71.1 ± 1.2	10(min)
2.0	100	0.2788	0.1462	1.1 × 10 ⁻⁴	4.7 × 10 ⁻¹⁴	0.9992	0.8908	1.91	2.3 × 10 ⁹	74.7 ± 0.7	0.5
	110	0.4485	0.1978	3.4 × 10 ⁻⁴	9.1 × 10 ⁻⁴	0.9998	0.9738	2.27	0.38	73.7 ± 0.6	0.5
	120	0.4945	0.2215	7.1 × 10 ⁻⁴	1.9 × 10 ⁻³	0.9994	0.9686	2.23	0.37	75.8 ± 1.5	15 (min)
	130	0.5669	0.2473	1.3 × 10 ⁻³	3.2 × 10 ⁻³	0.9999	0.9727	2.29	0.41	70.7 ± 2.1	15 (min)

the optimum reaction time to obtain the Y_{HMF} (t_{opt}) were listed in Table 4. As indicated by the results, t_{opt} decreased with an increase in reaction temperature in all the experiments. An increase in acid catalyst concentration up to 1.5 M also enhanced the HMF yield but further increase in catalyst concentration oppositely decreased the yield. H⁺ initiates the fructose dehydration, and three molecules of water were produced with the formation of one molecule of HMF according to reaction stoichiometry. This produced water could further react with the produced HMF due to the availability of free H⁺ in the system (see the possible reaction scheme provided in supporting information Fig. S1). High acid concentration (higher than the optimal point) increased the H⁺ density in the reaction system. The availability of these H⁺ could result in protonated water that is more reactive and promoted the rehydration of the produced HMF causing a decrease in maximum HMF yield. Hence, acid concentration and temperature were critical parameters for fructose dehydration. Therefore, with consideration of the HMF yield and selectivity, 120 °C was selected as the most feasible reaction temperature for *p*TSA catalyzed system. Du et al. (2019) reported the same kinetic behavior of homogeneous catalysts while comparing homogenous and heterogeneous acid-catalyzed dehydration of fructose in the water-dioxane solvent system. Concluded results indicate the higher HMF selectivity with homogeneous catalysts than a heterogeneous catalyst. However, the maximum obtained selectivity was (70%) much lower as compared to the results of this work.

To correlate the relationship of the observed rate constant with temperature and acid concentration, an extended Arrhenius equation can be used as followed:

$$k_{obs} = Ae^{\left(\frac{-E_a}{RT}\right)} C_{acid}^{\alpha} \quad (20)$$

where *A* is the pre-exponential factor; E_a is the activation energy; C_{acid} is the concentration of acid catalyst; and α is

the reaction order with respect to the acid concentration. By taking logarithm on both sides, the above equation can be transformed to:

$$\ln k_{obs} = \ln A - \frac{E_a}{RT} + \alpha \ln C_A \quad (21)$$

Therefore, the kinetic parameters for k_{1obs} and k_{2obs} can be determined by multiple linear regression based on the data listed in Table 5. The employed multiple linear regression generally showed satisfying goodness of fit with a determination coefficient (R²) of higher than 0.8. The objective reaction (fructose dehydration to form HMF) and primary side reaction (decomposition/condensation of fructose to form humin) had relatively low activation energies. However, the acid concentration showed a more significant effect on fructose condensation than dehydration, as reflected by the higher α value for k_{2obs} than k_{1obs}. Nevertheless, the fitted values for k_{3obs} and k_{4obs} varied in a very wide range of the order of magnitude. At low temperature, for example, 100 °C, the rate constants for rehydration and condensation reaction of HMF were very small (3–13 order of magnitude lower than that of k_{1obs} and k_{2obs}) so that these reactions actually could be neglected. However, these reactions become much more significant with greatly increased reaction rates (but still 2–3 order of magnitude lower than that of k_{1obs} and k_{2obs}) at a higher temperature such as 130 °C. Therefore, the estimated values for *A* and E_a by multi-linear regression would be extremely large for reaction (3) and (4). For example, the fitted *A* and E_a for reaction (3) were 1.102 × 10⁷⁷ and 611.2 kJ/mol. Such a high E_a actually is not normal and believable. It indicated that the temperature range of reaction used in the present work was not suitable for estimating the activation of HMF rehydration to form LA/FA and condensation to form humin. Actually, under the relatively optimal reaction temperature (120 °C), the rehydration and condensation of HMF could be neglected, because k_{3obs} and k_{4obs} were 2 order of magnitude lower than

Table 5 Estimated kinetic parameters for fructose dehydration to form HMF ($k_{1\text{obs}}$) and condensation to form humin ($k_{2\text{obs}}$) by multiple linear regression for *p*TSA and oxalic acid catalyzed dehydration of fructose in DMSO medium.

Catalyst	Observed rate constant	<i>A</i>	<i>E_a</i> (kJ/mol)	α	<i>R</i> ²
<i>p</i> TSA	$k_{1\text{obs}}$	1.431×10^4	33.75	0.1223	0.825
	$k_{2\text{obs}}$	3.231×10^2	24.94	0.4455	0.943
Oxalic acid	$k_{1\text{obs}}$	4.723×10^{11}	96.51	0.297	0.987
	$k_{2\text{obs}}$	7.152×10^8	78.39	0.579	0.963

$k_{1\text{obs}}$ and $k_{2\text{obs}}$. However, the results revealed that higher temperatures and high acid concentration definitely could greatly increase the side-reactions to decrease HMF selectivity and yield. Therefore, the rate constants for the main reactions of *p*TSA-catalyzed dehydration of fructose ($k_{1\text{obs}}$ and $k_{2\text{obs}}$) can be estimated by the following equations with respect to temperature and acid concentration:

$$k_{1\text{obs}} = 1.431 \times 10^4 \exp\left(-\frac{33750}{RT}\right) C_{\text{pTSA}}^{0.1223} \quad (22)$$

$$k_{2\text{obs}} = 3.231 \times 10^2 \exp\left(-\frac{24940}{RT}\right) C_{\text{pTSA}}^{0.4455} \quad (23)$$

3.3.2. Oxalic acid catalyzed system

Similar experiments were performed for oxalic acid catalyzed dehydration of fructose in DMSO medium. It was also apparently observed that temperature had significant effects on the kinetics of fructose conversion as well as the HMF yield. Compared with *p*TSA system, the fructose conversion had a much lower reaction rate for the oxalic acid system, especially at relatively low temperatures (e.g. 100 °C). For example, to achieve ~90% fructose conversion, 180 min was needed when the reaction was performed at 100 °C, while fructose conversion reached ~100% within 30 min at 130 °C. However, for *p*TSA catalyzed system, the complete conversion of fructose was achieved in 10–30 min even at 100 °C. The HMF yield steadily increased with reaction time and reached the maximum at 120 min. No sharp decrease in HMF yield and selectivity were observed for oxalic acid catalyzed system, probably due to its relatively weaker acidity. Therefore, it has appeared that the optimum temperature and reaction time were 130 °C and 2 h for oxalic acid-catalyzed dehydration of fructose.

The effects of initial fructose concentration on HMF yield were further investigated and compared with those obtained by *p*TSA catalyzed system. The maximum HMF yield was obtained at an initial concentration of fructose of 0.5 M and lowest at 2.0 M for both catalysts. The HMF yield was 80.86% for the oxalic acid system at 0.5 M fructose concentration, by the contrast of 90% for *p*TSA system. However, both catalysts showed similar HMF yield and selectivity (~75%) at 1.0 M initial fructose concentration. This phenomenon further indicated that the side reactions become more significant at higher fructose concentration.

The observed kinetics of oxalic acid catalyzed dehydration of fructose at an initial fructose concentration of 1.0 M with varied oxalic acid concentration (0.5–2.0 M) at different temperatures were further studied. The fitted observed rate constants are shown in Table 6. The results again illustrated that the developed kinetic models could well describe the kinetics of the fructose conversion and formation of HMF with *R*² gen-

erally being higher than 0.95. All the plots similarly illustrated that temperature showed a significant impact on the HMF yield and the formation of humin. However, the degradation of HMF (rehydration) seemed not so significant. This was proved by the fact that the HMF concentration increased with time but did not decrease significantly after reaching the maximum, even at a high reaction temperature (130 °C). The fitted kinetic rate constants listed in Table 6 showed that all of the rate constants increased with reaction temperature and oxalic acid concentration. The values of rate constants for dehydration of fructose to HMF ($k_{1\text{obs}}$) were in the same order of magnitude to those of the main side reaction ($k_{2\text{obs}}$). However, $k_{1\text{obs}}$ was larger than $k_{3\text{obs}}$ and $k_{4\text{obs}}$ by 8–12 orders of magnitude, indicating that the hydration and condensation of HMF in oxalic acid catalyzed system could be neglected. This could be proved by the experimental phenomenon that no LA/FA was detected in the system and only a small amount of LA was determined in a relatively long-time reaction at high temperature. For example, the LA concentration was only 0.003 M after oxalic acid catalyzed dehydration of 1.0 M fructose in DMSO for 180 min. This result further corroborated the high selectivity of DMSO system to reduce the degradation of HMF. Therefore, the reactions taking place in the system could be considered to only include the dehydration of fructose to form HMF and condensation of fructose to humin. The selectivity of fructose conversion listed in Table 6 suggested that 120–130 °C with 0.5 M acid concentration for 120 min reaction might be the optimal condition for oxalic acid system. Similarly, the HMF consumption selectivity data indicate an increase in HMF rehydration with temperature increase. Experimentally, the maximum HMF yield was obtained at 130 °C with 0.5 and 1.0 M acid concentration in 120 min; however, 1.5 M acid concentration gives the similar yield at 120 °C for reduced time of 60 min. Being similar to *p*TSA-catalyzed process, increase in temperature decreased the t_{opt} . Similarly, Eq. (21) was used to correlate the relationship of $k_{1\text{obs}}$ and $k_{2\text{obs}}$ with temperature and acid concentration by multiple linear regression, as shown in Table 5.

The results demonstrated that very satisfying goodness of fit was obtained with *R*² of 0.987 and 0.963 for $k_{1\text{obs}}$ and $k_{2\text{obs}}$, respectively. Both fructose dehydration and condensation in the oxalic acid system had higher activation energy and reaction order with respect to acid concentration than those in *p*TSA system, indicating that these reactions in the former system would be more sensitive to reaction temperature and catalyst concentration. Therefore, $k_{1\text{obs}}$ and $k_{2\text{obs}}$ for oxalic acid catalyzed system can be correlated by the following Eqs:

$$k_{1\text{obs}} = 4.723 \times 10^{11} \exp\left(-\frac{96510}{RT}\right) C_{\text{oxalic}}^{0.297} \quad (24)$$

Table 6 Kinetic parameters for oxalic acid catalyzed dehydration of fructose to HMF in DMSO medium at different temperatures with different acid catalyst concentration. The initial fructose concentration was 1.0 M.

Acid conc. (M)	T (°C)	Observed rate constant (min ⁻¹)				Goodness of Fit (R ²)		S _F	S _{HMF}	Max. Y _{HMF} (%)	t _{opt} (h)
		k _{1obs}	k _{2obs}	k _{3obs}	k _{4obs}	Fructose	HMF				
0.5	100	0.0129	0.00623	2.5 × 10 ⁻¹⁴	2 × 10 ⁻¹²	0.9566	0.9943	2.07	0.0125	63.3 ± 1.8	3
	110	0.0224	0.00835	1.7 × 10 ⁻¹⁴	8.6 × 10 ⁻¹⁴	0.9887	0.9802	2.68	0.198	72.6 ± 2.1	3
	120	0.0607	0.01423	1.4 × 10 ⁻¹⁴	1.3 × 10 ⁻¹⁴	0.9678	0.9359	4.27	1.08	79.2 ± 2.3	2.5
	130	0.1190	0.03769	6.0 × 10 ⁻¹⁴	2.9 × 10 ⁻¹⁴	0.9899	0.9038	3.16	2.1	84.1 ± 0.8	2
1	100	0.0145	0.0074	2.6 × 10 ⁻¹¹	2.4 × 10 ⁻¹²	0.9887	0.9783	1.96	0.108	67.7 ± 1.0	3
	110	0.0339	0.01295	7.5 × 10 ⁻¹¹	2.8 × 10 ⁻¹⁴	0.9808	0.9867	2.62	2.7 × 10 ³	74.4 ± 1.5	2
	120	0.0571	0.02485	2.5 × 10 ⁻¹¹	1.5 × 10 ⁻¹⁴	0.9852	0.9503	2.30	1.7 × 10 ³	75.5 ± 2.2	2
	130	0.1705	0.06505	2.9 × 10 ⁻¹⁰	2.2 × 10 ⁻¹⁴	0.9966	0.9569	2.62	1.3 × 10 ³	79.1 ± 1.2	2
1.5	100	0.0172	0.01160	9.85 × 10 ⁻¹⁰	9.6 × 10 ⁻¹¹	0.9658	0.9798	1.48	0.103	60.2 ± 1.6	3
	110	0.0391	0.02034	8.0 × 10 ⁻¹⁰	5.2 × 10 ⁻¹¹	0.9934	0.9319	1.92	0.154	69.3 ± 1.9	1.5
	120	0.0708	0.02612	6.1 × 10 ⁻¹⁰	4.9 × 10 ⁻¹⁰	0.9749	0.9669	2.71	1.24	80.1 ± 0.9	1
	130	0.1781	0.07214	1.2 × 10 ⁻¹⁰	3.2 × 10 ⁻¹⁰	0.9879	0.8018	2.47	0.375	74.6 ± 2.1	1
2	100	0.0184	0.01172	1.5 × 10 ⁻¹⁰	4.4 × 10 ⁻¹⁵	0.9879	0.9698	1.57	3.3 × 10 ⁴	62.5 ± 3.1	2
	110	0.0384	0.01981	6.3 × 10 ⁻¹⁰	2.7 × 10 ⁻¹³	0.9798	0.9325	1.94	2.3 × 10 ³	76.9 ± 2.6	2
	120	0.0746	0.03289	5.9 × 10 ⁻¹⁰	3.8 × 10 ⁻¹³	0.9715	0.8993	2.27	1.5 × 10 ³	76.1 ± 0.5	2
	130	0.1954	0.08244	2.4 × 10 ⁻¹⁰	3.7 × 10 ⁻¹³	0.9824	0.9408	2.37	6.48 × 10 ²	76.6 ± 1.3	1

$$k_{2\text{obs}} = 7.152 \times 10^8 \exp\left(-\frac{78390}{RT}\right) C_{\text{oxalic}}^{0.579} \quad (25)$$

A comparison of kinetic data with published results seems appropriate although it is very tough because the reaction environment is rarely comparable. Moreover, it must be taken into contemplation that mostly the apparent rate constants are sturdily dependent on the catalyst, reaction medium, and temperature. As shown in supporting information Table S2 on a summary of activation energy for acid-catalyzed dehydration of fructose by various catalysts in different reaction mediums, the obtained activation energy indeed varied in a wide range of 60–170 kJ/mol. For example, Asghari and Yoshida (2007) investigated fructose dehydration to HMF with HCl as a catalyst and proposed a kinetic model involving the reaction between fructose and HMF to produce by-products with an activation energy of 160.6 kJ/mol. Likewise, the activation energy determined by Bicker et al. (2005) was 80 kJ/mol when sulfuric acid (0.01 M) was used in supercritical methanol and supercritical acetic acid for fructose dehydration. This activation energy was close to that of the system with oxalic acid as the catalyst in this work. However, for *p*TSA-catalyzed system in this work, the activation energy was much lower. This was probably because the *p*TSA concentration was high so that the reaction was not so sensitive toward reaction temperature. Nevertheless, these results revealed the fact that the apparent rate constants and the activation energy of HMF formation by fructose dehydration were strongly dependent on the reaction system. Anyway, the obtained results illustrated that the developed kinetic models could be well applied for describing the kinetics of *p*TSA or oxalic acid catalyzed dehydration of fructose to produce HMF in DMSO system.

A comparison of the HMF yield obtained in this work with reported results is shown in supporting information Table S3. It can be known that high (usually near 100%) conversion of fructose generally could be obtained but the HMF yield varied

in a wide range and greatly dependent on the fructose concentration, solvent, catalysts used, reaction temperature and time. The highest HMF yield (98%) was reported when a glucose-based sulfonated carbonaceous catalyst was used (Wang et al., 2013). However, the reaction system was relatively small with a lower initial fructose concentration (0.28 M). In this work, 80–90% HMF yield was obtained by the optimization of process parameters and kinetic modeling in a relatively larger reaction system (50 ml), which was among the high level of reported HMF yields. The developed kinetic model thus could be further used as a tool to optimize and control the process.

4. Conclusions

Several organic acids including *p*TSA and some dicarboxylic acids such as oxalic acid, maleic acid, malonic acid and succinic acid were employed as catalysts to catalyze the dehydration of fructose to HMF in water or organic solvent medium under mild condition (100–130 °C). Quantitative comparison of the fructose conversion and HMF yield was performed based on observed kinetic modeling. An observed kinetic model considering the dehydration of fructose to HMF, condensation of fructose, and HMF to humin and rehydration of HMF to LA/FA was developed. It was found that the developed observed kinetic models could well describe the kinetics of fructose conversion and the formation of HMF with satisfying goodness of fit for both water and DMSO reaction systems. The rate constants for fructose dehydration and condensation increased with the acidity strength (pK_{a1}) of the acid catalysts, indicating that the reactions were initiated by protonation. *p*TSA and oxalic acid have been selected as the best catalysts to obtain high HMF yield. In the water medium, the fructose dehydration and condensation have similar rate constants, leading to selectivity for fructose conversion of about 1. The rehydration reaction of HMF had lower rate

constant, but still comparable with those for fructose dehydration and condensation. Several high-boiling point solvents were tested as reaction medium in order to improve the HMF selectivity and yield. DMSO was found to be the most effective. In DMSO system, the rehydration of HMF could be greatly reduced leading to a significant increase in the selectivity. Moreover, the HMF rehydration and condensation actually could be neglected, especially for the oxalic acid catalyzed system. The determined observed activation energy for fructose conversion to HMF and humin in DMSO medium was determined to be 33.75 and 24.94 kJ/mol for *p*TSA-catalyzed system, and 96.51 and 78.39 kJ/mol for oxalic acid-catalyzed system, respectively. Under the respective optimum condition, HMF yields of 90.2% and 84.1% were obtained for *p*TSA and oxalic acid catalyzed systems, respectively.

Acknowledgments

This work was supported by National Natural Science Foundation of China (No. 21878176).

Appendix A. Supplementary material

Supplementary data to this article can be found online at <https://doi.org/10.1016/j.arabjc.2020.08.019>.

References

- Akien, G.R., Qi, L., Horváth, I.T., 2012. Molecular mapping of the acid catalysed dehydration of fructose. *Chem. Commun.* 48, 5850–5852. <https://doi.org/10.1039/c2cc31689g>.
- Antal, M.J., Mok, W.S.L., Richards, G.N., 1990. Mechanism of formation of 5-(hydroxymethyl)-2-furaldehyde from d-fructose and sucrose. *Carbohydr. Res.* 199, 91–109. [https://doi.org/10.1016/0008-6215\(90\)84096-D](https://doi.org/10.1016/0008-6215(90)84096-D).
- Antonetti, C., Fulignati, S., Licursi, D., Raspolli Galletti, A.M., 2019. Turning point towards the sustainable production of HMF in water: metal salts for its synthesis from fructose and inulin. *ACS Sustain. Chem. Eng.* 7, 6830–6838. <https://doi.org/10.1021/acssuschemeng.8b06162>.
- Asghari, F.S., Yoshida, H., 2007. Kinetics of the decomposition of fructose catalyzed by hydrochloric acid in subcritical water: Formation of 5-hydroxymethylfurfural, levulinic, and formic acids. *Ind. Eng. Chem. Res.* 46, 7703–7710. <https://doi.org/10.1021/ie061673e>.
- Bicker, M., Kaiser, D., Ott, L., Vogel, H., 2005. Dehydration of d-fructose to hydroxymethylfurfural in sub- and supercritical fluids. *J. Supercrit. Fluids* 36, 118–126. <https://doi.org/10.1016/J.SUPFLU.2005.04.004>.
- Chaudhary, K., Subodh, Prakash, K., Mogha, N.K., Masram, D.T., 2020. Fruit waste (Pulp) decorated CuO NFs as promising platform for enhanced catalytic response and its peroxidase mimics evaluation. *Arab. J. Chem.* 13, 4869–4881. <https://doi.org/10.1016/j.arabjc.2019.09.007>.
- Chen, L., Dou, J., Ma, Q., Li, N., Wu, R., Bian, H., Yelle, D.J., Vuorinen, T., Fu, S., Pan, X., Zhu, J., 2017. Rapid and near-complete dissolution of wood lignin at $\leq 80^\circ\text{C}$ by a recyclable acid hydrotrope. *Sci. Adv.* 3, <https://doi.org/10.1126/sciadv.1701735> e1701735.
- Clarke, C.J., Tu, W.-C., Levers, O., Brö, A., Hallett, J.P., 2018. Green and sustainable solvents in chemical processes. *Chem. Rev.* 118, 747–800. <https://doi.org/10.1021/acs.chemrev.7b00571>.
- Dalessandro, E.V., Pliego, J.R., 2018. Fast screening of solvents for simultaneous extraction of furfural, 5-hydroxymethylfurfural and Levulinic acid from aqueous solution using SMD solvation free energies. *J. Braz. Chem. Soc.* 29, 430–434. <https://doi.org/10.21577/0103-5053.20170140>.
- de Souza, R.L. et al, 2012. 5-hydroxymethylfurfural (5-HMF) production from hexoses: limits of heterogeneous catalysis in hydrothermal conditions and potential of concentrated aqueous organic acids as reactive solvent system. *Challenges* 3, 212–232. <https://doi.org/10.3390/challe3020212>.
- Desir, P., Saha, B., Vlachos, D.G., Ghatta, A. Al, Wilton-Ely, J.D.E. T., Hallett, J.P., 2019. Ultrafast flow chemistry for the acid-catalyzed conversion of fructose. *Energy Environ. Sci.* 12, 2463–2475. <https://doi.org/10.1039/c9ee01189g>.
- Du, M., Agrawal, A.M., Chakraborty, S., Garibay, S.J., Limvorapitux, R., Choi, B., Madrahimov, S.T., Nguyen, S.T., 2019. Matching the activity of homogeneous sulfonic acids: the fructose-to-HMF conversion catalyzed by hierarchically porous sulfonic-acid-functionalized porous organic polymer (POP) catalysts. *ACS Sustain. Chem. Eng.* 7, 8126–8135. <https://doi.org/10.1021/acssuschemeng.8b05720>.
- Espenson, 1981. *Chemical Kinetics and Reaction Mechanisms*. McGraw-Hill, New York.
- Gajula, S., Inthumathi, K., Arumugam, S.R., Srinivasan, K., 2017. Strategic designing on selection of solvent systems for conversion of biomass sugars to furan derivatives and their separation. *ACS Sustain. Chem. Eng.*, 5373–5381 <https://doi.org/10.1021/acssuschemeng.7b00681>.
- Galkin, K.I., Ananikov, V.P., 2019. When will 5-hydroxymethylfurfural, the “Sleeping Giant” of sustainable chemistry, awaken? *ChemSusChem* 12, 2976–2982. <https://doi.org/10.1002/cssc.201900592>.
- Garcés, D.G., Díaz, E., Ordóñez, S.O., Garcés, D., Díaz, E., Ordóñez, S., 2017. Aqueous phase conversion of hexoses into 5-hydroxymethylfurfural and Levulinic acid in the presence of hydrochloric acid: mechanism and kinetics. *I EC Res.* 56, 5221–5230. <https://doi.org/10.1021/acs.iecr.7b00952>.
- Gawade, A.B., Yadav, G.D., 2018. Microwave assisted synthesis of 5-ethoxymethylfurfural in one pot from d-fructose by using deep eutectic solvent as catalyst under mild condition. *Biomass Bioenergy* 117, 38–43. <https://doi.org/10.1016/J.BIOMBIOE.2018.07.008>.
- Heo, J.B., Lee, Y.S., Chung, C.H., 2019. Raw plant-based biorefinery: A new paradigm shift towards biotechnological approach to sustainable manufacturing of HMF. *Biotechnol. Adv.* <https://doi.org/10.1016/j.biotechadv.2019.107422>.
- Hu, Z., Liu, B., Zhang, Z., Chen, L., 2013. Conversion of carbohydrates into 5-hydroxymethylfurfural catalyzed by acidic ionic liquids in dimethyl sulfoxide. *Ind. Crops Prod.* 50, 264–269. <https://doi.org/10.1016/j.indcrop.2013.07.014>.
- Kimura, H., Nakahara, M., Matubayasi, N., 2013. Solvent effect on pathways and mechanisms for d-fructose conversion to 5-hydroxymethyl-2-furaldehyde: In situ ^{13}C NMR study. *J. Phys. Chem. A* 117, 2102–2113. <https://doi.org/10.1021/jp312002h>.
- Körner, P., Jung, D., Kruse, A., 2018. The effect of different Brønsted acids on the hydrothermal conversion of fructose to HMF. *Green Chem.* 20, 2231–2241. <https://doi.org/10.1039/C8GC00435H>.
- Mellmer, M.A., Sanpitakseree, C., Demir, B., Bai, P., Ma, K., Neurock, M., Dumesic, J.A., 2018. Solvent-enabled control of reactivity for liquid-phase reactions of biomass-derived compounds. *Nat. Catal.* 1, 199–207. <https://doi.org/10.1038/s41929-018-0027-3>.
- Nikbin, N., Caratzoulas, S., Vlachos, D.G., 2012. A first principles-based microkinetic model for the conversion of fructose to 5-hydroxymethylfurfural. *ChemCatChem* 4, 504–511. <https://doi.org/10.1002/cctc.201100444>.
- Rosatella, A.A., Simeonov, S.P., Frade, R.F.M.M., Afonso, C.A.M. M., 2011. 5-Hydroxymethylfurfural (HMF) as a building block

- platform: Biological properties, synthesis and synthetic applications. *Green Chem.* 13, 754–793. <https://doi.org/10.1039/c0gc00401d>.
- Sajid, M., Zhao, X., Liu, D., 2018. Production of 2,5-furandicarboxylic acid (FDCA) from 5-hydroxymethylfurfural (HMF): recent progress focusing on the chemical-catalytic routes. *Green Chem.* 20, 5427–5453. <https://doi.org/10.1039/c8gc02680g>.
- Steinbach, D., Kruse, A., Sauer, J., Vetter, P., 2018. Sucrose is a promising feedstock for the synthesis of the platform chemical hydroxymethylfurfural. *Energies* 11, 645. <https://doi.org/10.3390/en11030645>.
- Sun, X., Zhao, X., Du, W., Liu, D., Xiaoying, S., Xuebing, Z., Wei, D., Dehua, L., 2011. Kinetics of formic acid-autocatalyzed preparation of performic acid in aqueous phase *. *Chinese J. Chem. Eng.* 19,. [https://doi.org/10.1016/S1004-9541\(11\)60078-5](https://doi.org/10.1016/S1004-9541(11)60078-5) 964971.
- Takeuchi, Y., Fangming, A.E., Kazuyuki, J.A., Ae, T., Enomoto, H., 2008. Acid catalytic hydrothermal conversion of carbohydrate biomass into useful substances. *J. Mater. Sci.* 43, 2472–2475. <https://doi.org/10.1007/s10853-007-2021-z>.
- Thananattananachon, T., Rauchfuss, T.B., 2010. Efficient route to hydroxymethylfurans from sugars via transfer hydrogenation. *ChemSusChem* 3, 1139–1141. <https://doi.org/10.1002/cssc.201000209>.
- van Dam, H.E., Kieboom, A.P.G.G., van Bekkum, H., 1986. The Conversion of Fructose and Glucose in Acidic Media: Formation of Hydroxymethylfurfural. *Starch - Stärke* 38, 95–101. <https://doi.org/10.1002/star.19860380308>.
- Van Putten, R.J., van der Waal, J.C., de Jong, E., Rasrendra, C.B., Heeres, H.J., de Vries, J.G., 2013. Hydroxymethylfurfural, a versatile platform chemical made from renewable resources. *Chem. Rev.* 113, 1499–1597. <https://doi.org/10.1021/cr300182k>.
- Villanueva, N.I., Marzalletti, T.G., 2018. Mechanism and kinetic parameters of glucose and fructose dehydration to 5-hydroxymethylfurfural over solid phosphate catalysts in water. *Catal. Today* 302, 100–107. <https://doi.org/10.1016/J.CATTOD.2017.04.049>.
- Wang, L., Guo, H., Xie, Q., Wang, J., Hou, B., Jia, L., Cui, J., Li, D., 2019. Conversion of fructose into furfural or 5-hydroxymethylfurfural over HY zeolites selectively in γ -butyrolactone. *Appl. Catal. A Gen.* 572, 51–60. <https://doi.org/10.1016/J.APCATA.2018.12.023>.
- Wang, J., Ren, J., Liu, X., Lu, G., Wang, Y., 2013. High yield production and purification of 5-hydroxymethylfurfural. *Am. Inst. Chem. Eng. AIChE J.* 59, 2558–2566. <https://doi.org/10.1002/aic>.
- Wang, C., Zhang, L., Zhou, T., Chen, J., Xu, F., 2017. Synergy of Lewis and Bronsted acids on catalytic hydrothermal decomposition of carbohydrates and corncob acid hydrolysis residues to 5-hydroxymethylfurfural. *Nat. Sci. Rep.* 7, 40908–40917. <https://doi.org/10.1038/srep40908>.
- Werpy, T., Peterson, G., 2004. Top Value Added Chemicals from Biomass, vol. 1. National Renewable Energy Laboratory (NREL), US department of energy, Alexandria, Virginia.
- Wrigstedt, P., Keskinvälti, J., Repo, T., 2016. Microwave-enhanced aqueous biphasic dehydration of carbohydrates to 5-hydroxymethylfurfural. *RSC Adv.* 6, 18973–18979. <https://doi.org/10.1039/C5RA25564C>.
- Yoshida, F.S.A.H., 2006. Acid-catalyzed production of 5-hydroxymethyl furfural from D-fructose in subcritical water. *Ind. Eng. Chem. Res.* 45, 2163–2173. <https://doi.org/10.1021/ie051088y>.
- Yu, I.K.M., Tsang, D.C.W., 2017. Conversion of biomass to hydroxymethylfurfural: A review of catalytic systems and underlying mechanisms. *Bioresour. Technol.* 238, 716–732. <https://doi.org/10.1016/j.biortech.2017.04.026>.
- Zhang, Z., Huber, G.W., 2018. Catalytic oxidation of carbohydrates into organic acids and furan chemicals. *Chem. Soc. Rev.* 47, 1351–1390. <https://doi.org/10.1039/C7CS00213K>.
- Zhang, X., Murria, P., Jiang, Y., Xiao, W., Kenttämä, H.I., Abu-Omar, M.M., Mosier, N.S., 2016. Maleic acid and aluminum chloride catalyzed conversion of glucose to 5-(hydroxymethyl) furfural and levulinic acid in aqueous media. *Green Chem.* 18, 5219–5229. <https://doi.org/10.1039/c6gc01395c>.
- Zhang, L., Xi, G., Yu, K., Yu, H., Wang, X., 2017. Furfural production from biomass-derived carbohydrates and lignocellulosic residues via heterogeneous acid catalysts. *Ind. Crops Prod.* 98, 68–75. <https://doi.org/10.1016/J.INDCROP.2017.01.014>.
- Zhao, X., Li, S., Wu, R., Liu, D., 2017. Organosolv fractionating pretreatment of lignocellulosic biomass for efficient enzymatic saccharification: chemistry, kinetics, and substrate structures. *Biofuels. Bioprod. Biorefining* 11, 567–590. <https://doi.org/10.1002/bbb.1768>.
- Zuo, M., Le, K., Li, Z., Jiang, Y., Zeng, X., Tang, X., Sun, Y., Lin, L., 2017. Green process for production of 5-hydroxymethylfurfural from carbohydrates with high purity in deep eutectic solvents. *Ind. Crops Prod.* 99, 1–6. <https://doi.org/10.1016/j.indcrop.2017.01.027>.